Supplementary of

Reactive species formed upon interaction of water with fine particulate matter from remote forest and polluted urban air

H. Tong *et al.*

Correspondence to: Haijie Tong (h.tong@mpic.de).

Influence of $PM_{2.5}$ extract concentration on the radical yield.

To assess the influence of the $PM_{2.5}$ extract concentrations on our results, we compared the mass-specific radical yields by different concentration of Beijing $PM_{2.5}$ extracts. We found the yield difference is on average for 37% among all extract samples. However, we did not see clear trend from low to high concentration of $PM_{2.5}$ extracts. Then we showed the $PM_{2.5}$ extract concentrations of each sample as well as the radical yields by different concentration of $PM_{2.5}$ extracts in Figure S1. Figures S1a-1c indicate that $PM_{2.5}$ extract concentrations of Hyytiälä and Mainz samples have narrower range distribution than Beijing samples. Figure S1d and 1e showed that radical yields by 500 μg mL^{-1} fine $PM_{2.5}$ overlapped the yields by 250-6400 μg mL^{-1} PM. Thus, the concentration of the $PM_{2.5}$ extracts has small impact on our results about RS yields. To evaluate the influence of $PM_{2.5}$ extract concentrations on the relative yields of different radicals, we measured the relative yields of different radicals by Beijing $PM_{2.5}$ (n=3) in 250, 500, and 1000 μg mL^{-1} $PM_{2.5}$ extracts. We found the relative yields of $^{\bullet}OH$, $O_2^{\bullet-}$, C- and O-centered organic radicals have standard deviations of ~10%, ~9%, ~2%, and ~2%, respectively.

Estimation of the abundance of organic hydroperoxides and humic-like substances in $PM_{2.5}$

Based on the compiled abundance of humic-like substances in $PM_{2.5}$ (Table S3), we obtained an averaged value of 7%, and we assumed that 15% of these $PM_{2.5}$-bound humic-like substances are extractable humic acid-like substances (Katsumi et al., 2019). Given that the concentration of $PM_{2.5}$ in aqueous extracts in this study ranged from 250 to 6500 μg mL^{-1}, thus the estimated concentration of humic acid-like substances typically ranged from 3 to 70 μg mL^{-1}. We assumed that 75% of the $PM_{2.5}$-bound humic-like substances are attributable to humic acid-like substances, thus the estimated concentration of extractable fulvic acid-like substances typically ranged from 15 to 350 μg mL^{-1}. To simulate the RS formation by Mainz and Beijing $PM_{2.5}$, we used 4 μg mL^{-1} humic acid standard. To investigate the influence of humic-like substances on the RS formation by Fenton-like reactions, we used 6-180 μg mL^{-1} humic or fulvic acid for surrogate mixture measurements.

To estimate the abundance of organic hydroperoxide in ambient $PM_{2.5}$, we assumed that the mass fractions of SOA in Hyytiälä, Mainz, and Beijing $PM_{2.5}$ were 60%, 25%, and 15%, respectively (Jimenez

et al., 2009). We also assumed that 2%, 2%, and 1% of Hyytiälä, Mainz, and Beijing SOA mass are attributable to organic hydroperoxides (Tong et al., 2018), which was assumed to have an averaged molecular weight of 300 g moL^{-1} (Docherty et al., 2005). In this case, the estimated concentration of organic hydroperoxides in the $PM_{2.5}$ extracts in this study was 5-35 μM. To simulate the RS formation by Hyytiälä, Mainz, and Beijing fine $PM_{2.5}$, we used 50, 25, and 0 μM cumene hydroperoxide (CHP), respectively. To investigate the RS yield of Fenton-like reactions, we used 50-100 μM CHP.

H_2O_2 yield of PM from other sources

The air sample volume-specific and mass-specific H_2O_2 yields as well as total RS yields of fine PM from other sites that different from Hyytiälä, Mainz, and Beijing are shown in Figure S4 and Table S5. Therein the H_2O_2 yields were measured using *p*-hydroxyphenylacetic acid (PHOPAA) as probe, and the total RS yields were measured using dichlorofluorescin (DCFH) assay as probe (Lazrus et al., 1985;Wang and Joseph, 1999;Kalyanaraman et al., 2012). Figure S4a shows that the air sample volume-specific H_2O_2 yields of fine PM from CRC-AES and different districts of UCLA exhibit a positive correlation with the concentration of $PM_{2.5}$ (R^2=0.60). In contrast, the mass-specific H_2O_2 yields exhibit no correlation with the $PM_{2.5}$ concentration (R^2=0.02, Figure S4b). Moreover, the DCFH-based total RS yields were overall higher than the H_2O_2 (Table S5), agreeing with this study.

Influence of H_2O_2 on the radical yield of Fenton-like reactions

We investigated the influence of H_2O_2 concentration on the radical yield of Fenton-like reactions initiated by mixtures comprising 100 μM CHP, 300 μM Fe^{2+}, 11 μg mL^{-1} HA, and 79 μg mL^{-1} FA. Figure S5a shows that as the concentration of H_2O_2 is increased from 0 to 300 μM, the concentration of total radicals increase from ~8.0 to ~18.4 μM, with the RF of $^{\bullet}OH$ and O-centered organic radicals increase from ~18 to ~69% and from ~7 to ~26% (Figure S5b), confirming the enhanced radical formation through Fenton-like reactions (Gligorovski et al., 2015). In contrast, the RF of C-centered radicals and $O_2^{\bullet-}$ decrease from ~25 to ~2% and from ~51 to ~3%, reflecting a plausible conversion of C-centered radicals to O-centered organic radicals via oxidation pathways (Chevallier et al., 2004;Tong et al., 2016). Thus, H_2O_2 can significantly

influence the total and relative yields of different types of radicals by Fenton-like reactions, and humic-like substances may co-mediate the radical formation.

Influence of HA and FA on the radical yields of Fenton-like reactions initiated by Cu^{2+}

Figure S7a shows that the concentration of radicals formed by Cu^{2+} and cumene hydroperoxide (CHP) mixtures exhibited a positive correlation with the concentration of Cu^{2+}. However, the Cu^{2+} played a less effective role than Fe^{2+} in initiating Fenton-like reactions via radical formation pathways, with 300 μM Cu^{2+} and 50 μM CHP produced ~1.8 μM radicals.

Figure S7b shows that as the concentration of Cu^{2+} increased from 15 to 75 μM, the RF of $^{\bullet}OH$ and $O_2^{\bullet-}$ decreased from ~44% to ~18% and from ~1.6% to ~0.1%. However, the RF of C- and O-centered organic radicals increased from~39% to ~61% and from ~15% to ~21%, respectively. As the concentration of Cu^{2+} is increased further to 150 and 300 μM, the RF of $^{\bullet}OH$, $O_2^{\bullet-}$, C- and O-centered organic radicals varied slightly, reflecting a low reactivity of Cu^{2+} with CHP.

Figure S7c shows that concentration of radicals formed by reactions of 100 μM CHP with 300 μM Cu^{2+} and HA decreased from ~2.3 to ~1.8 μM as the increasing of HA concentration from 0 to 180 μg mL^{-1}. This might mainly be associated with the low catalytic effect of Cu^{2+} in initiating Fenton-like reactions (Figure S5a). Beyond this, humic-like substances have been found to exhibit strong copper-binding ability (Kogut and Voelker, 2001), and 8-fold more Cu^{2+} than Fe^{2+} ions from Melpitz (Germany) PM were expected to be complexed by humic-like substances (Scheinhardt et al., 2013). We thus inferred that the Cu-HA complex might significantly influence the reactivity of Cu^{2+} in Fenton-like reactions. Finally, partial of the radical yield decay in Figure S7a might be caused by the antioxidant effect of HA (Aeschbacher et al., 2012). Figure S7d shows that as the concentration of HA increased from 6 to 180 μg mL^{-1}, the RF of $^{\bullet}OH$ and O-centered organic radicals increased from ~17 to ~44% and from ~16 to ~28%, respectively. The RF variation of $^{\bullet}OH$, C- and O-centered organic radicals in Figure S7d had a different trend from the results in Figure 6d, reflecting different impacts of HA on Cu and Fe initiated Fenton-like reactions. Compared to the

increasing RF of $^{\bullet}OH$ and O-centered organic radicals, the RF of C-centered radicals decreased from ~66 to ~28%, and the RF of $O_2^{\bullet-}$ only varied slightly between 0.8 and 1.5%.

Figure S7e shows that the radical yields of the mixtures consisting of 100 μM CHP, 300 μM Cu^{2+}, and FA only varied from ~0.9 to ~0.4 μM as the increasing FA concentration from 6 to 180 μg mL^{-1}, which may mainly be associated with the low catalytic effect of Cu^{2+} as well as the formation of Cu-FA complexes. Figure S7f indicates that as the concentration of FA increased from 0 to 180 μg mL^{-1}, the RF of C-centered radicals steeply increased from ~57 to ~89%, whereas the RF of O-centered organic radicals and $^{\bullet}OH$ exhibited overall decrease from ~25% and ~16% to ~3%.

Table S1. **Sampling information.**

City	Location	Sampler	Flow rate (L min^{-1})	Sampling time (h) [a]	Sampling period	Sample numbers
Hyytiälä	61.51°N, 24.17°E	Dekati® PM10 impactor (Finland)	30	48-72	31 May-19 July 2017	11
Mainz	49.99°N, 8.23°E	MOUDI (MSP corporation, USA) [b]	30	24-54	22 Aug.-17 Nov. 2017 23-31 Aug. 2018	11
Beijing	116.31°E, 39.99°N	$PM_{2.5}$ sampler (TH-16, Tianhong company, China)	30	5-24	20 Dec. 2016-13 Jan. 2017 6 Nov. 2017-17 Jan. 2018	20

[a] The sampling time is for one filter

[b] MOUDI: Micro-Orifice Uniform Deposition Impactor (122R)

92 **Table S2. The range of hyperfine coupling constants that used to fit the BMPO adducts.**

Spin adduct	Hyperfine coupling constant (G)		
	a_{N}	a_H^{β}	a_H^{γ}
BMPO-OH1	12-16	11-12	0.5-0.9
BMPO-OH2	14-15	13-14	0.6-0.7
BMPO-OOH1	13-14	8-10	—
BMPO-OOH2	13-14	11-13	—
BMPO-C-centered radicals	14-16	21-23	—
BMPO-O-centered organic radicals	14-16	17-18	—

93

Table S3. Compiled abundance of humic-like substances in ambient $PM_{2.5}$.

Location	Time/event	$PM_{2.5}$ ($\mu g\ m^{-3}$)	humic-like substances ($\mu g\ m^{-3}$)	humic-like substances /$PM_{2.5}$ (%)	Reference
Lanzhou	Winter	120.47	7.24	6.0	(Tan et al., 2016)
Lanzhou	Summer	34.12	2.15	6.3	(Tan et al., 2016)
Lanzhou	Annual	77.29	4.7	6.1	(Tan et al., 2016)
Lanzhou	Haze	182.08	10.06	5.5	(Tan et al., 2016)
Lanzhou	No-haze	51.65	3.49	6.8	(Tan et al., 2016)
Lanzhou	Snow	80.69	4.62	5.7	(Tan et al., 2016)
PRD[a]	Annual 2007-2008	49	4.9	10.0	(Lin et al., 2010)
Guangzhou	Annual 2009	56	4.8	8.6	(Kuang et al., 2015)
Beijing	Winter 2011	108	8.9	8.2	(Lang et al., 2017)
Beijing	Summer	98	5.5	5.9	(Li et al., 2019)
Beijing	Autumn	58	5.6	9.4	(Li et al., 2019)
Beijing	Winter	150	12.3	7.9	(Li et al., 2019)
Beijing	Spring	120	6.5	4.8	(Li et al., 2019)
Average		91.2	6.2	7.0	

PRD: Pearl River Delta Region in China

Table S4. The yields of different types of radicals and concentrations of different water-soluble transition metal species in $PM_{2.5}$ extracts.

Location	Radicals (pmol m^{-3})				Water-soluble transition metals (pmol m^{-3})				
	$^{\bullet}OH$	C-centered	O-centered organic	$O_2^{\bullet-}$	Fe	Mn	Cu	V	Ni
Hyytiälä	0.4 ± 0.2	2.2 ± 1.4	0.1 ± 0.1	0.02 ± 0.01	26.0 ± 16.0	4.9 ± 4.8	3.1 ± 1.2	2.5 ± 1.7	0.04 ± 0.01
Mainz	2.1 ± 1.3	1.8 ± 0.7	0.2 ± 2	0.1 ± 0.1	269.0 ± 113.0	28.0 ± 12.0	55.0 ± 17.0	2.9 ±0.8	1.2 ± 0.4
Beijing	3.6 ± 2.6	2.5 ± 1.7	0.3 ± 0.2	0.2 ± 0.3	(3300.0 ± 2300.0)	640.0 ± 531.0	452.0 ± 385.0	23.0 ± 23.0	51.0 ± 25.0
Location	Radicals (pmol μg^{-1})				Water-soluble transition metals (pmol μg^{-1})				
	$^{\bullet}OH$	C-centered	O-centered organic	$O_2^{\bullet-}$	Fe	Mn	Cu	V	Ni
Hyytiälä	0.08 ± 0.004	0.5 ± 0.2	0.03 ± 0.01	0.01 ± 0.01	5.5 ± 1.5	1.0 ± 0.5	0.7 ± 0.3	0.5 ± 0.2	0.01 ± 0.003
Mainz	0.2 ± 0.1	0.1 ± 0.07	0.02 ± 0.02	0.01 ± 0.01	18.0 ± 4.9	1.9 ± 0.7	3.9 ± 0.6	0.2 ± 0.03	0.08 ± 0.03
Beijing	0.04 ± 0.04	0.02 ± 0.02	0.003 ± 0.002	0.002 ± 0.002	20.0 ± 7.0	4.5 ± 2.6	2.3 ± 0.4	0.2 ± 0.2	0.5 ± 0.5

Table S5. Statistic of H_2O_2 or RS yields of ambient PM at different locations.

Sampling site	PM type	PM (μg m^{-3})	Sampling time	Method	Analyte	H_2O_2 or RS (pmol m^{-3})	H_2O_2 or RS (pmol μg^{-1})	Reference
Hyytiälä	$PM_{2.5}$	5 ± 2	Jun-Jul 2017	MAK165	H_2O_2	10 ± 8	1.9 ± 0.9	This study
UCLA Pacific coast	Fine	13 ± 10	May 2014-Jan 2015	PHOPAA+HRP	H_2O_2	12 ± 9	1.0 ± 0.9	(Arellanes et al., 2006)
MPI-C at Mainz	$PM_{1.8}$	16 ± 2	Aug-Sep 2017	MAK165	H_2O_2	47 ± 17	3.3 ± 1.1	This study
UCLA	$PM_{2.5}$	16 ± 7	2009-2010	PHOPAA+HRP	H_2O_2	47 ± 21	3.0 ± 2.0	(Wang et al., 2012)
CRC-AES, UC Riverside	$PM_{2.5}$	19 ± 6	Jun-Aug 2008	PHOPAA+HRP	H_2O_2	$(2.7 \pm 2.1) \times 10^2$	1.4 ± 1.6	(Wang et al., 2012)
UCLA freeway site	Fine	23 ± 8	Jan-May 2004	PHOPAA+HRP	H_2O_2	17 ± 90	0.7 ± 1.1	(Arellanes et al., 2006)
UCLA Pacific coast	Coarse	26 ± 15	Jul 2004	PHOPAA+HRP	H_2O_2	31 ± 9	1.2 ± 0.6	(Arellanes et al., 2006)
UCLA freeway site	Coarse	27 ± 33	Jul 2004	PHOPAA+HRP	H_2O_2	15 ± 9	0.6 ± 0.3	(Arellanes et al., 2006)
UC Riverside campus	$PM_{2.5}$	39 ± 22	Aug 2005	PHOPAA+HRP	H_2O_2	$(1.2 \pm 1.1) \times 10^3$	28.0 ± 20.0	(Wang et al., 2012)
UCLA campus	Coarse	46 ± 22	Aug 2005	PHOPAA+HRP	H_2O_2	$(5.0 \pm 2.4) \times 10^2$	14.1 ± 9.4	(Wang et al., 2010)
UCLA upwind Riverside	Coarse	97 ± 27	Jun-Aug 2008	PHOPAA+HRP	H_2O_2	$(1.0 \pm 0.4) \times 10^3$	10.9 ± 5.3	(Wang et al., 2010)
Beijing	$PM_{2.5}$	201 ± 160	Dec 2016- Jan 2017	MAK165	H_2O_2	190 ± 120	3.4 ± 5.6	This study
Taipei	Coarse	7.5± 2.8	Jul-Sep 2000	DCFH+HRP	RS	64 ± 33	8.5 ± 11.8	(Hung and Wang, 2001)
Bern	$PM_{2.5}$	10 ± 5	Nov 2014	DCFH+HRP	RS	$(4.9 \pm 2.9) \times 10^2$	50	(Zhou et al., 2018)

Atlanta	$PM_{2.5}$	10.5 ± 3.2	12-17 Jul 2012	DCFH+HRP	RS	$(1.6 \pm 0.2) \times 10^2$	14.8 ± 4.5	(King and Weber, 2013)
Atlanta	$PM_{2.5}$	11.5 ± 4.3	8-31 May 2012	DCFH+HRP	RS	$(2.6 \pm 0.1) \times 10^2$	22.6 ± 3.0	(King and Weber, 2013)
Atlanta	$PM_{2.5}$	13.2 ± 4.8	8-29 Jun 2012	DCFH+HRP	RS	$(1.4 \pm 0.1) \times 10^2$	10.6 ± 1.9	(King and Weber, 2013)
Atlanta	$PM_{2.5}$	13.2 ± 5.4	3-31 Jul 2012	DCFH+HRP	RS	$(2.4 \pm 0.1) \times 10^2$	18.2 ± 1.8	(King and Weber, 2013)
London	$PM_{2.5}$	5-28	not reported	DCFH+HRP	RS	$(0.4\text{-}2.4) \times 10^4$	not reported	(Wragg et al., 2016)
Singapore (campus)	$PM_{2.5}$	19 ± 2	Dec 2005	DCFH+HRP	RS	$(5.7 \pm 0.7) \times 10^3$	0.3	(See et al., 2007)
Taipei	$PM_{3.2}$	31 ± 15	Jul-Sep 2000	DCFH+HRP	RS	$(5.4 \pm 0.5) \times 10^2$	17.6 ± 29.2	(Hung and Wang, 2001)
Singapore (curbside)	$PM_{2.5}$	33 ± 6	Dec 2005	DCFH+HRP	RS	$(1.5 \pm 0.2) \times 10^4$	460	(See et al., 2007)
Milan (traffic site)	TSP	50 ± 7	July 2013	DCFH+HRP	RS	$(1.4 \pm 0.7) \times 10^2$	2.73 ± 1.29	(Perrone et al., 2016)
Milan (low emission zone)	TSP	52 ± 19	Oct 2013	DCFH+HRP	RS	$(2.0 \pm 1.1) \times 10^2$	3.74 ± 1.41	(Perrone et al., 2016)
Milan (traffic site)	TSP	57 ± 19	Oct 2013	DCFH+HRP	RS	$(2.4 \pm 1.3) \times 10^2$	4.02 ± 1.77	(Perrone et al., 2016)
Beijing	$PM_{2.5}$	5-110	Aug-Sep 2015	DCFH+HRP	RS	$(0.2\text{-}3.6) \times 10^4$	not reported	(Huang et al., 2018)
Beijing	$PM_{2.5}$	74 ± 58	Dec 2014	DCFH+HRP	RS	$(1.3 \pm 0.5) \times 10^4$	179.6 ± 87.8	(Huang et al., 2016)
Beijing	$PM_{2.5}$	79 ± 59	Apr 2015	DCFH+HRP	RS	$(5.8 \pm 2.6) \times 10^3$	73.6 ± 43.4	(Huang et al., 2016)
Milan (traffic site)	TSP	129± 60	Jan-Feb 2013	DCFH+HRP	RS	$(3.6 \pm 0.8) \times 10^2$	2..99 ± 1.52	(Perrone et al., 2016)
Rubidoux, CA	$PM_{2.5}$	not reported	Jul 2003	DCFH+HRP	RS	$(4.7 \pm 0.4) \times 10^3$	not reported	(Venkatachari et al., 2005)
Rochester, NY	$PM_{2.5}$	not reported	Aug 2009	DCFH+HRP	RS	$(8.3 \pm 2.2) \times 10^3$	not reported	(Wang et al., 2011)

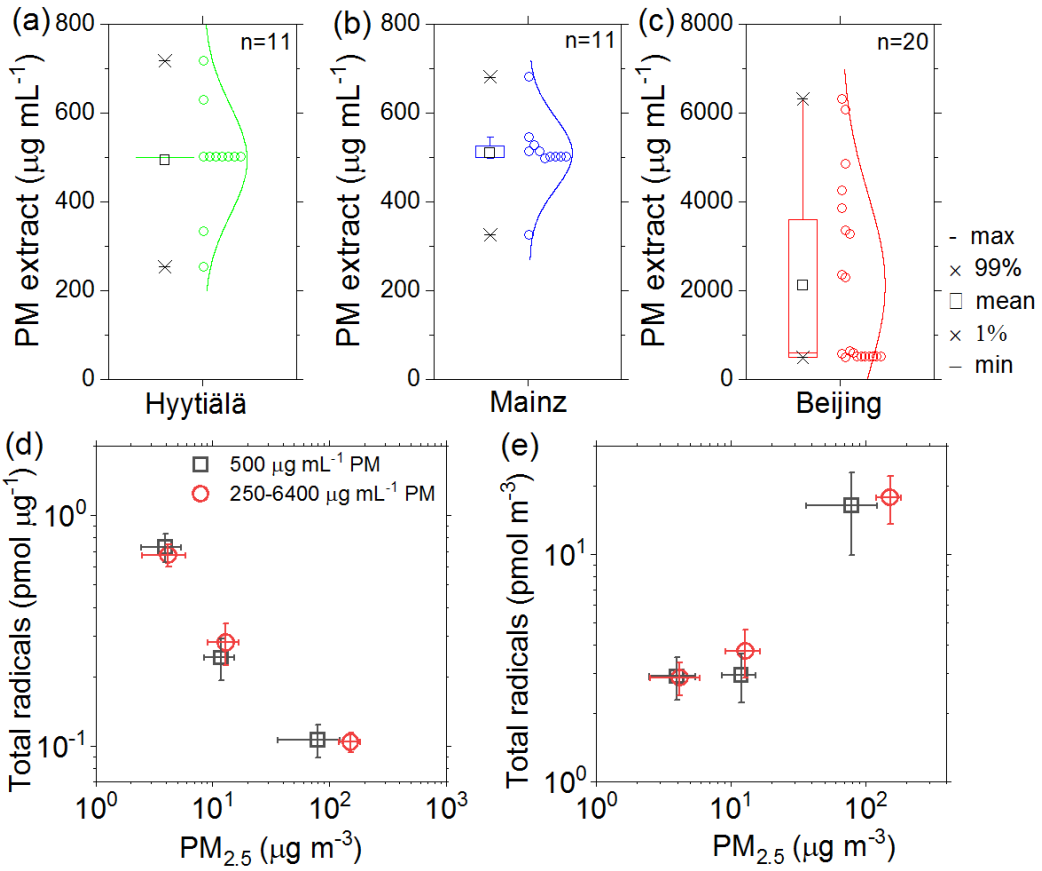

Figure S1. (a-c) Concentrations of $PM_{2.5}$ in aqueous extracts of each filter samples. (d) Mass-specific radical yields by different concentrations of $PM_{2.5}$ in water versus the concentration of ambient $PM_{2.5}$ in air. (e) Air sample volume-specific radical yields by different concentrations of PM versus the concentration of ambient $PM_{2.5}$. The error bars denote the standard errors (11-20 samples per location).

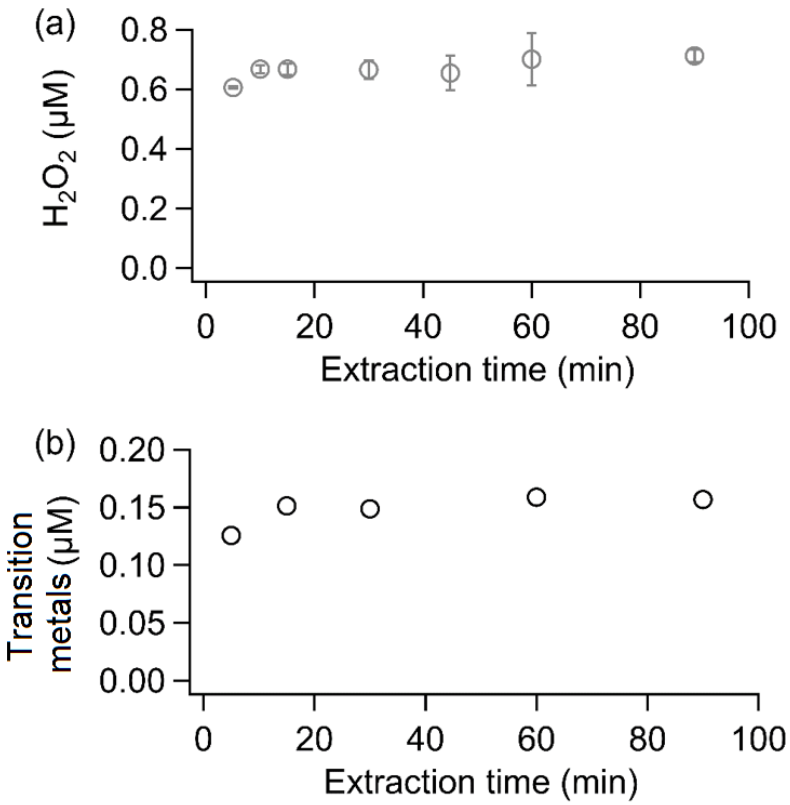

106

107 **Figure S2.** (a) Temporal evolution of H_2O_2 concentration in water extracts during the extraction process.
108 Error bars represent standard deviation of duplicate measurements. (b) Temporal evolution of water-soluble
109 transition metal concentration in water extracts during the extraction process. The H_2O_2 and transition metal
110 concentrations became constant after ~15 min's extraction. The filter used for these tests was collected at
111 Mainz from 25 to 27 Oct. 2017.

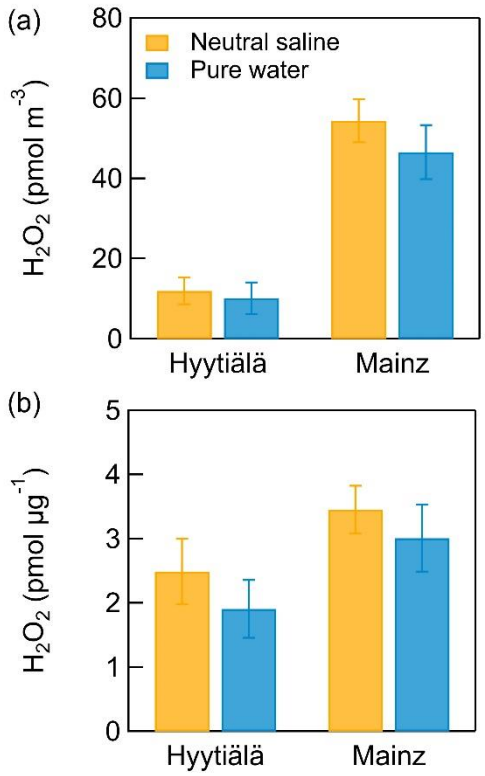

Figure S3. (a) Air sample volume-specific and (b) mass-specific H_2O_2 yield of Hyytiälä and Mainz fine PM in neutral saline (yellow column) and pure water (blue column). The error bars represent standard deviations of mean (11-12 samples per location).

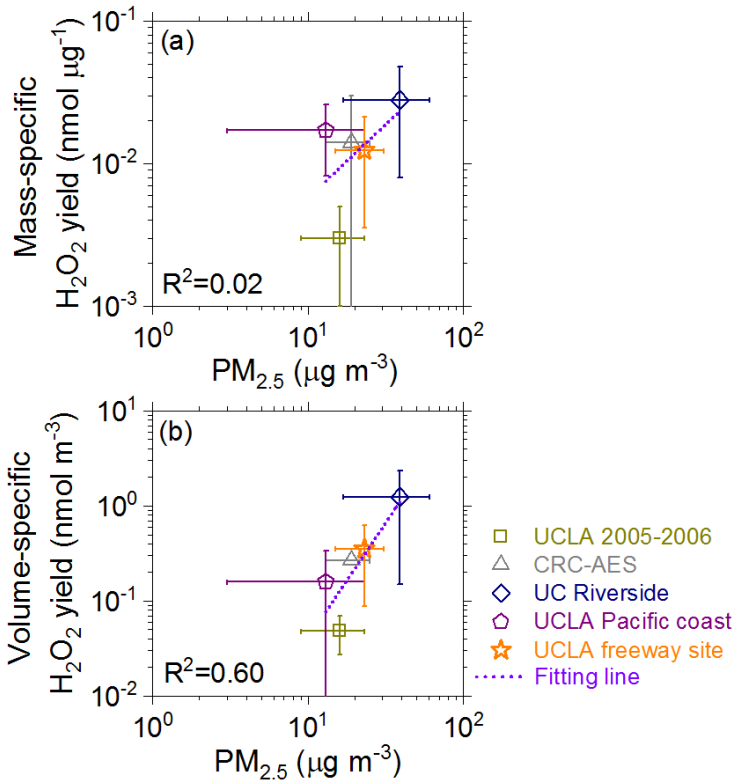

116

117 **Figure S4.** (a) Mass-specific and (b) air sample volume-specific H_2O_2 and RS yields of PM from different

118 sites. The error bars represent standard deviation.

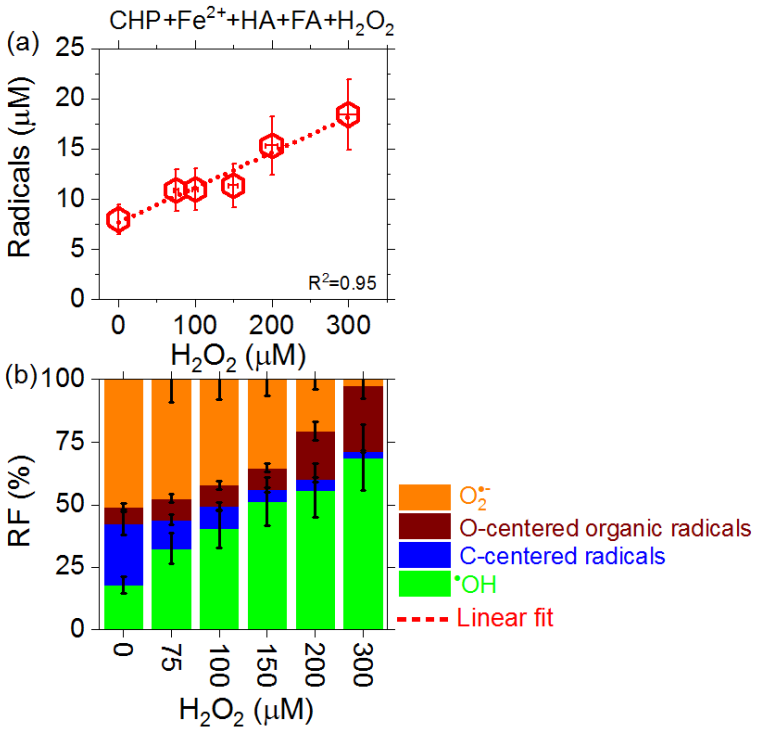

119

120 **Figure S5.** (a) Total radical yield and (b) relative fractions (RF) of individual radicals observed in aqueous

121 surrogate mixtures of CHP, Fe^{2+}, HA, FA, and H_2O_2. CHP: 100 μM. Fe^{2+}: 300 μM. HA: 100 μg mL^{-1}. FA:

122 80 μg mL^{-1}. H_2O_2: 0-300 μM. The error bars represent uncertainties of signal integration of EPR spectra

123 (for y-axis) or experimental uncertainties of the solution concentration (for x-axis).

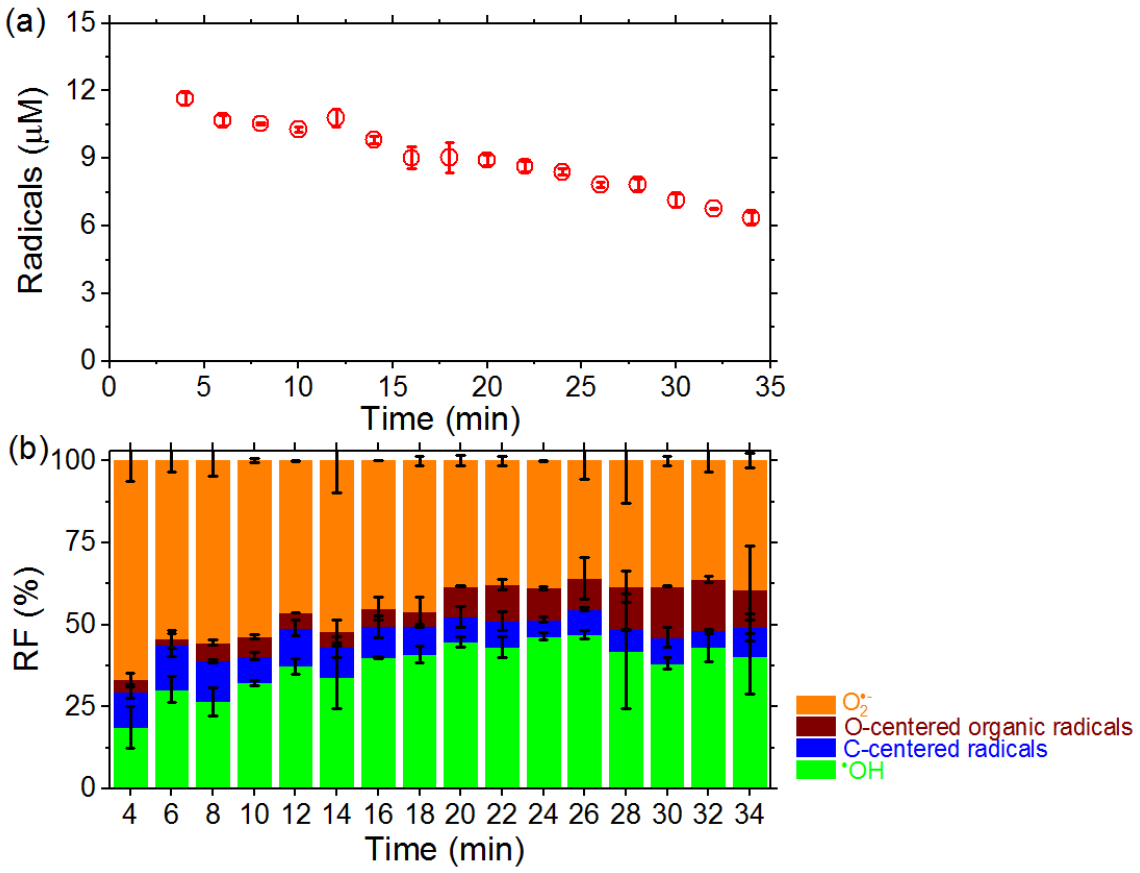

Figure S6. (a) Temporal evolution of total radical concentration and (b) relative fractions (RF) of individual radical species in aqueous mixtures of 100 μM CHP and 300 μM Fe^{2+}. Error bars represent standard deviation of duplicate measurements.

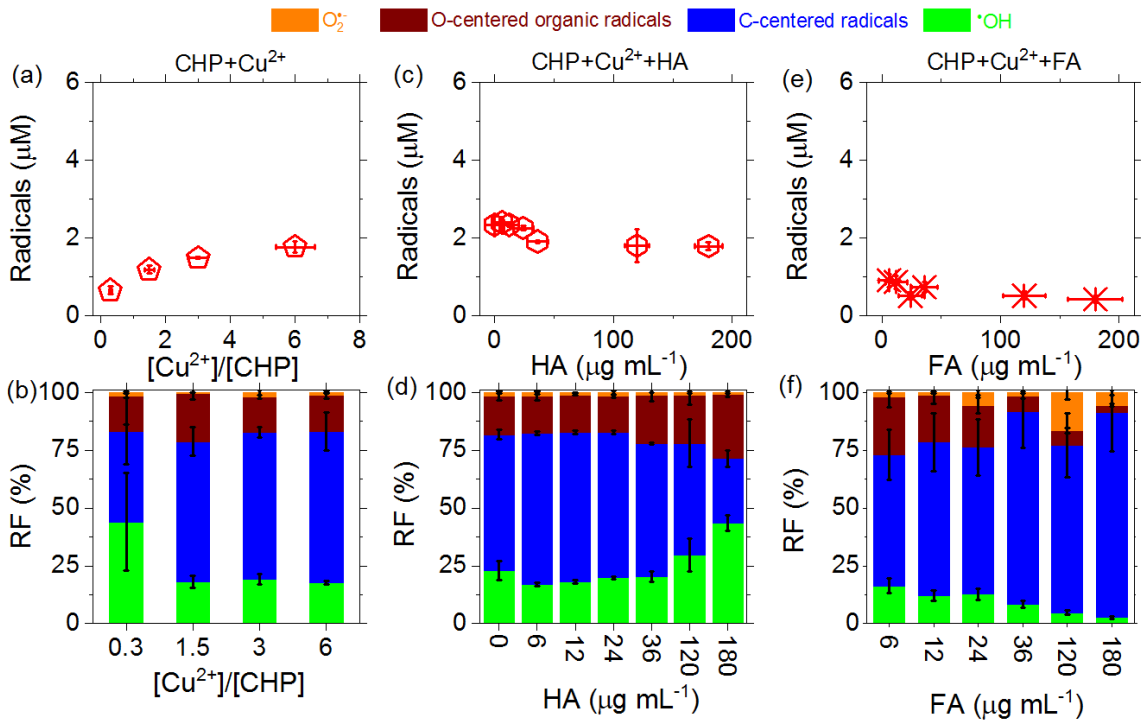

Figure S7. (a, c, e) Concentration of totally formed radicals and (b, d, f) RF of individual radicals in aqueous mixtures comprising CHP, Cu^{2+}, HA, or FA. The concentration of CHP in (a) and (b) is 50 μM. The concentrations of CHP and Cu^{2+} in (c-f) are 100 and 300 μM. The error bars in (a) to (d) represent standard errors of the mean (3 -5 samples per data point, a, b). The error bars for x- and y-axis in (e) and (f) represent experimental uncertainties of the solution concentration and signal integration of EPR spectra, respectively.

References

Aeschbacher, M., Graf, C., Schwarzenbach, R. P., and Sander, M.: Antioxidant properties of humic substances, Environ. Sci. Technol., 46, 4916-4925, 2012.

Arellanes, C., Paulson, S. E., Fine, P. M., and Sioutas, C.: Exceeding of Henry's law by hydrogen peroxide associated with urban aerosols, Environ. Sci. Technol., 40, 4859-4866, 2006.

Chevallier, E., Jolibois, R. D., Meunier, N., Carlier, P., and Monod, A.: "Fenton-like" reactions of methylhydroperoxide and ethylhydroperoxide with Fe^{2+} in liquid aerosols under tropospheric conditions, Atmos. Environ., 38, 921-933, 2004.

Docherty, K. S., Wu, W., Lim, Y. B., and Ziemann, P. J.: Contributions of organic peroxides to secondary aerosol formed from reactions of monoterpenes with O_3, Environ. Sci. Technol., 39, 4049-4059, 2005.

Gligorovski, S., Strekowski, R., Barbati, S., and Vione, D.: Environmental implications of hydroxyl radicals ($^{\bullet}OH$), Chem. Rev., 115, 13051-13092, 2015.

Huang, W., Zhang, Y., Zhang, Y., Zeng, L., Dong, H., Huo, P., Fang, D., and Schauer, J. J.: Development of an automated sampling-analysis system for simultaneous measurement of reactive oxygen species (ROS) in gas and particle phases: GAC-ROS, Atmos. Environ., 134, 18-26, 2016.

Huang, W., Fang, D., Shang, J., Li, Z., Zhang, Y., Huo, P., Liu, Z., Schauer, J. J., and Zhang, Y.: Relative impact of short-term emissions controls on gas and particle-phase oxidative potential during the 2015 China Victory Day Parade in Beijing, China, Atmos. Environ., 183, 49-56, 2018.

Hung, H.-F., and Wang, C.-S.: Experimental determination of reactive oxygen species in Taipei aerosols, J. Aerosol Sci., 32, 1201-1211, 2001.

Jimenez, J. L., Canagaratna, M., Donahue, N., Prevot, A., Zhang, Q., Kroll, J. H., DeCarlo, P. F., Allan, J. D., Coe, H., and Ng, N.: Evolution of organic aerosols in the atmosphere, Science, 326, 1525-1529, 2009.

Kalyanaraman, B., Darley-Usmar, V., Davies, K. J., Dennery, P. A., Forman, H. J., Grisham, M. B., Mann, G. E., Moore, K., Roberts II, L. J., and Ischiropoulos, H.: Measuring reactive oxygen and nitrogen species with fluorescent probes: challenges and limitations, Free Radic. Biol. Med., 52, 1-6, 2012.

Katsumi, N., Miyake, S., Okochi, H., Minami, Y., Kobayashi, H., Kato, S., Wada, R., Takeuchi, M., Toda, K., and Miura, K.: Humic-like substances global levels and extraction methods in aerosols, Environ. Res. Lett., 17, 1023-1029, 2019.

King, L., and Weber, R.: Development and testing of an online method to measure ambient fine particulate reactive oxygen species (ROS) based on the 2',7'-dichlorofluorescin (DCFH) assay, Atmos. Meas. Tech., 6, 1647-1658, 2013.

Kogut, M. B., and Voelker, B. M.: Strong copper-binding behavior of terrestrial humic substances in seawater, Environ. Sci. Technol., 35, 1149-1156, 2001.

Kuang, B. Y., Lin, P., Huang, X., and Yu, J. Z.: Sources of humic-like substances in the Pearl River Delta, China: positive matrix factorization analysis of $PM_{2.5}$ major components and source markers, Atmos. Chem. Phys., 15, 1995-2008, 2015.

Lang, J., Zhang, Y., Zhou, Y., Cheng, S., Chen, D., Guo, X., Chen, S., Li, X., Xing, X., and Wang, H.: Trends of $PM_{2.5}$ and chemical composition in Beijing, 2000–2015, Aerosol Air Qual. Res., 17, 412-425, 2017.

Lazrus, A. L., Kok, G. L., Gitlin, S. N., Lind, J. A., and McLaren, S. E.: Automated fluorimetric method for hydrogen peroxide in atmospheric precipitation, Anal. Chem., 57, 917-922, 1985.

Li, X., Han, J., Hopke, P. K., Hu, J., Shu, Q., Chang, Q., and Ying, Q.: Quantifying primary and secondary humic-like substances in urban aerosol based on emission source characterization and a source-oriented air quality model, Atmos. Chem. Phys., 19, 2327-2341, 2019.

Lin, P., Engling, G., and Yu, J.: Humic-like substances in fresh emissions of rice straw burning and in ambient aerosols in the Pearl River Delta Region, China, Atmos. Chem. Phys., 10, 6487-6500, 2010.

Perrone, M. G., Zhou, J., Malandrino, M., Sangiorgi, G., Rizzi, C., Ferrero, L., Dommen, J., and Bolzacchini, E.: PM chemical composition and oxidative potential of the soluble fraction of particles at two sites in the urban area of Milan, Northern Italy, Atmos. Environ., 128, 104-113, 2016.

Scheinhardt, S., Müller, K., Spindler, G., and Herrmann, H.: Complexation of trace metals in size-segregated aerosol particles at nine sites in Germany, Atmos. Environ., 74, 102-109, 2013.

See, S., Wang, Y., and Balasubramanian, R.: Contrasting reactive oxygen species and transition metal concentrations in combustion aerosols, Environ. Res., 103, 317-324, 2007.

Tan, J., Xiang, P., Zhou, X., Duan, J., Ma, Y., He, K., Cheng, Y., Yu, J., and Querol, X.: Chemical characterization of humic-like substances (HULIS) in $PM_{2.5}$ in Lanzhou, China, Sci. Total Environ., 573, 1481-1490, 2016.

Tong, H., Arangio, A. M., Lakey, P. S., Berkemeier, T., Liu, F., Kampf, C. J., Brune, W. H., Pöschl, U., and Shiraiwa, M.: Hydroxyl radicals from secondary organic aerosol decomposition in water, Atmos. Chem. Phys., 16, 1761-1771, 2016.

Tong, H., Lakey, P. S., Arangio, A. M., Socorro, J., Shen, F., Lucas, K., Brune, W. H., Pöschl, U., and Shiraiwa, M.: Reactive oxygen species formed by secondary organic aerosols in water and surrogate lung fluid, Environ. Sci. Technol., 52, 11642-11651, 2018.

Venkatachari, P., Hopke, P. K., Grover, B. D., and Eatough, D. J.: Measurement of particle-bound reactive oxygen species in Rubidoux aerosols, J. Atmos. Chem., 50, 49-58, 2005.

Wang, H., and Joseph, J. A.: Quantifying cellular oxidative stress by dichlorofluorescein assay using microplate reader, Free Radic. Biol. Med., 27, 612-616, 1999.

Wang, Y., Arellanes, C., Curtis, D. B., and Paulson, S. E.: Probing the source of hydrogen peroxide associated with coarse mode aerosol particles in Southern California, Environ. Sci. Technol., 44, 4070-4075, 2010.

Wang, Y., Hopke, P. K., Sun, L., Chalupa, D. C., and Utell, M. J.: Laboratory and field testing of an automated atmospheric particle-bound reactive oxygen species sampling-analysis system, J. Toxicol., 2011, 419476, 2011.

Wang, Y., Arellanes, C., and Paulson, S. E.: Hydrogen peroxide associated with ambient fine-mode, diesel, and biodiesel aerosol particles in Southern California, Aerosol Sci. Technol., 46, 394-402, 2012.

Wragg, F., Fuller, S. J., Freshwater, R., Green, D. C., Kelly, F. J., and Kalberer, M.: An automated online instrument to quantify aerosol-bound reactive oxygen species (ROS) for ambient measurement and health-relevant aerosol studies, Atmos. Meas. Tech., 9, 4891-4900, 2016.

Zhou, J., Bruns, E. A., Zotter, P., Stefenelli, G., Prévôt, A. S., Baltensperger, U., El-Haddad, I., and Dommen, J.: Development, characterization and first deployment of an improved online reactive oxygen species analyzer, Atmos. Meas. Tech., 11, 65-80, 2018.